Effect of Chromium Content on Mechanical Properties of V-*x*Cr-4Ti-0.15Y Alloys

Takeshi MIYAZAWA, Takeo MUROGA and Yoshimitsu HISHINUMA

National Institute for Fusion Science, Gifu, JAPAN

(Received: 16 September 2014 / Accepted: 19 January 2015)

A combined effect of purification and yttrium (Y) addition was investigated to improve impact properties of high-chromium V-*x*Cr-4Ti alloys. Tensile tests and Charpy impact tests were carried out by using miniaturized specimens. V-10Cr-4Ti-0.15Y alloy had ultimate tensile stress (UTS) at 700 °C and yield stress (YS) approximately equal to and higher than those of V-4Cr-4Ti alloy, respectively. V-10Cr-4Ti-0.15Y alloy had more favorable impact properties than those of previous V-*x*Cr-4Ti alloys with $x > 9$ wt.%. It is proposed that purification and Y addition may suppress the formation of the large Ti-rich complexes with carbon, oxygen and nitrogen which act as crack initiation sites.

Keywords: low-activation materials, blanket structural materials, solution hardening of Cr, tensile properties, impact properties

1. Introduction

Vanadium (V)-based alloys nominally containing Chromium (Cr) of 4 wt.% and Titanium (Ti) of 4 wt.% are regarded as advanced blanket structural materials for fusion reactors because they potentially have low-induced activation characteristics, high-temperature strength, and high thermal stress factors [1]. The upper and lower limits for the operation temperature of V-4Cr-4Ti alloy are determined by high-temperature strength and irradiation embrittlement, which are currently assumed to be around 700 and 450 °C, respectively [2]. It is well known that solid solution and precipitation of interstitial impurities of Carbon (C), Oxygen (O) and Nitrogen (N) strongly affect the mechanical and irradiation properties in V-4Cr-4Ti alloys [3, 4]. The previous study clarified that the large and small precipitates were identified as Ti-rich and Ti-C-O complexes, respectively [5]. V-4Cr-4Ti alloy is annealed at 1000 °C to remove the interstitial impurities from the alloy matrix by the formation of these Ti precipitates. Oxygen, however, tends to remain in the matrix compared with C and N even after the annealing, and can enhance irradiation hardening [6]. Therefore, yttrium (Y) with stronger chemical affinity with O than Ti is added to remove O further from the matrix. V-4Cr-4Ti-0.15Y alloy has exhibited a reduction of irradiation hardening and an improvement of ductility in tensile tests after neutron irradiation around 400 °C, and is expected to expand the lower temperature operation limit [7, 8]. However, V-4Cr-4Ti-0.15Y alloy has also exhibited a reduction of high-temperature strength due to the loss of hardening by the dynamic strain aging (DSA) effect [9]. With the Y addition, the formation of Cottrell atmospheres, composed of interstitial C, N and O locking dislocations, was suppressed, and resulting in the loss of DSA.

Cr is known to increase the strength of V at high temperatures. Increasing Cr content relative to V-4Cr-4Ti-0.15Y alloy is considered to be an effective method in order to compensate for the reduction of high-temperature strength due to the reduction in interstitial impurities by the scavenging effect of Y. However, excess Cr addition can lead to loss of ductility and degradation of workability [10]. The influence of the interstitial impurities on the Cr effects is not known.

In this study, V-*x*Cr-4Ti-0.15Y alloys with high-Cr contents are fabricated in order to improve the impact properties of V-*x*Cr-4Ti alloys without degrading the high-temperature strength. A combined effect of purification and Y addition is investigated by the evaluation of tensile properties and impact properties.

2. Experimental

Results of chemical analysis for V alloys used in this study are shown in Table 1. V-4Cr-4Ti alloy is the reference alloy, so-called NIFS-HEAT-2, which was fabricated by electron beam melting and vacuum arc re-melting in 166 kg-scale [11, 12]. Three alloys of V-*x*Cr-4Ti-0.15Y (x = 4, 6, 10 wt.%) were fabricated by 15 kg-scale levitation melting at Daido Steel Co. Ltd. [13, 14]. Figure 1 shows fabrication process of V-*x*Cr-4Ti-0.15Y (x = 4, 6, 10 wt.%) alloys. These ingots were cut and machined to remove a cavity formed at the bottom and the periphery. After the cutting and machining, the size of these ingots was 140 mm in diameter and 45 mm in height. Small blocks with 30 x 30 x 20 mm^3 were cut from V-10Cr-4Ti-0.15Y ingot in order to investigate the

author's e-mail: miyazawa.takeshi@LHD.nifs.ac.jp

Table 1 Chemical composition of the alloys (wt.%)

Code	V	Cr	Ti	Y	C	N	O
V-4Cr-4Ti	bal.	4.02	4.15	<0.01	0.012	0.009	0.012
V-4Cr-4Ti-0.15Y	bal.	4.23	4.17	0.11	0.011	0.009	0.009
V-6Cr-4Ti-0.15Y	bal.	6.21	4.16	0.08	0.013	0.011	0.0095
V-10Cr-4Ti-0.15Y	bal.	9.93	3.90	0.09	0.011	0.014	0.007

workability. Each ingot was canned into a 304 type stainless steel container by electron-beam welding. The canned ingot was hot-forged in the range of 900-1150 ºC. After forging, cold rolling was performed to obtain various thickness of plates. V-4Cr-4Ti-0.15Y and V-6Cr-4Ti-0.15Y alloys had such a favorable workability that no intermediate annealing was required through the several steps of cold rolling. However, V-10Cr-4Ti-0.15Y alloy had an unfavorable workability since the intermediate annealing (1000 ºC for 3.6 ks) was required in order to obtain plates by cold rolling.

The sheet specimens for Vickers hardness tests were cut from the plates with 1 mm in thickness. The sheet specimens were mechanically and electrolytically polished, followed by annealing at the range of 600-1100 ºC for 3.6 ks in a vacuum better than 1 x 10^{-4} Pa. The hardness tests were carried out at 500 gf for 30 s at room temperature (RT). The hardness was calculated by averaging the hardness obtained from ten indents. Miniature tensile specimens with a gauge size of 1.2 x 5 x 0.25 mm^3, called SSJ specimens, were punched from the plates with 0.25 mm in thickness. Miniaturized Charpy specimens were machined from plates with 4 mm in thickness for V-4Cr-4Ti-0.15Y and V-6Cr-4Ti-0.15Y alloys, and from plates with 2 mm in thickness for V-10Cr-4Ti-0.15Y alloy. The Charpy specimens had dimensions of 1.5 x 1.5 x 20 mm^3, a notch angle of 30º, and a notch depth of 0.3 mm, so that ligament size was 1.2 mm. Charpy and tensile specimens were annealed at 1000 ºC for 7.2 ks for V-4Cr-4Ti alloy, and at 950 ºC for 3.6 ks for V-*x*Cr-4Ti-0.15Y alloys. Tensile tests were performed from RT to 800 ºC in a vacuum better than 1 x 10^{-4} Pa. The initial strain rate was 6.67 x 10^{-4} s^{-1}. Charpy impact tests were conducted from -196 ºC to RT using the instrumented Charpy impact testers at International Research Center for Nuclear Materials Science, Tohoku University and NIFS. The crosshead speed of Charpy impact tests was 5 m/s. Fracture surfaces were analyzed using scanning electron microscopy (SEM).

3. Results

Figure 2 shows hardness recovery as a function of the final annealing temperature after cold rolling. Every hardness is the average of ten indents corresponding sample at different surface position. The hardness has a minimum between 900 and 1000 ºC. The minimum values increased with increasing Cr content.

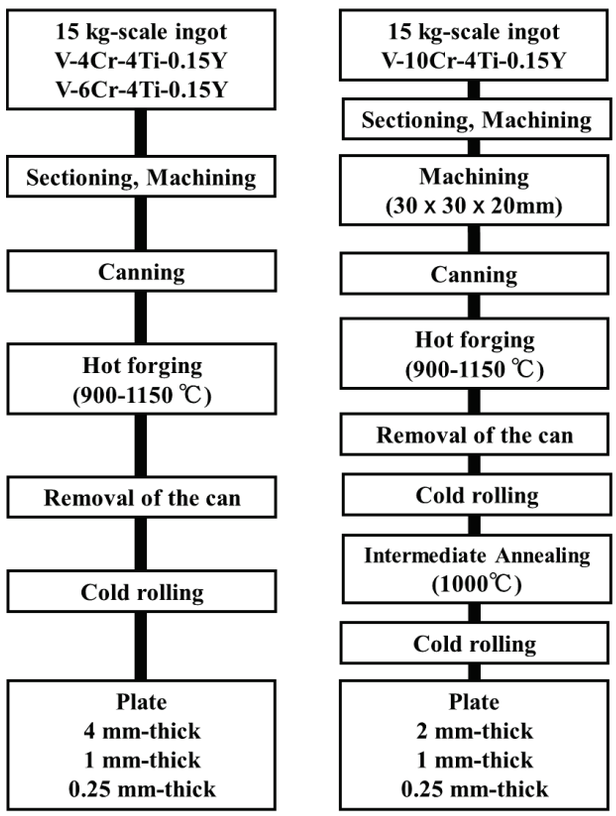

Fig. 1. Fabrication process of V-*x*Cr-4Ti-0.15Y (*x* = 4, 6, 10 wt.%) alloys.

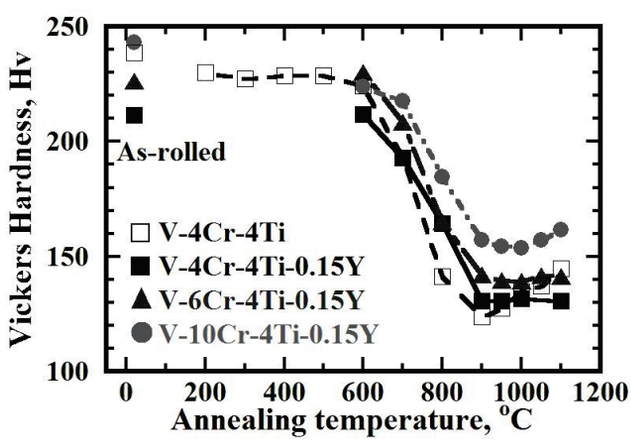

Fig. 2. Recovery of hardness as a function of final annealing after cold rolling. Open squares represent hardness for V-4Cr-4Ti alloy [5].

Figures 3 and 4 show the dependence of tensile strength and elongation on test temperatures, respectively. Tensile strength for V-*x*Cr-4Ti-0.15Y alloys increased with increasing Cr content. It must be noted that there was a difference in the dependence of ultimate tensile strength (UTS) and total elongation (TE) on test temperature between V-4Cr-4Ti alloy and V-*x*Cr-4Ti-0.15Y alloys. Between 600 to 700 ºC, UTS for V-4Cr-4Ti alloy remained almost constant, while that for V-*x*Cr-4Ti-0.15Y alloys decreased. V-10Cr-4Ti-0.15Y alloy has UTS at 700 ºC approximately equal to that of V-4Cr-4Ti alloy. TE for V-*x*Cr-4Ti-0.15Y alloys increased remarkably above 600 ºC. Figure 5 shows tensile stress-strain curves for the alloys at 700 ºC. Tensile tests for V-4Cr-4Ti alloy at 700 ºC were carried out twice in order to confirm the reproducibility of serrations. The deformation behavior of V-4Cr-4Ti alloy during tensile tests typically within temperatures ranging 300 to 750 ºC was shown to exhibit DSA, which is manifested by oscillations in the flow stress as serrations on the stress-strain curves [9]. Serrations for V-*x*Cr-4Ti-0.15Y alloys disappeared at 700 ºC as shown in Fig. 5. The decrease in strength and increase in elongation at 700 ºC for V-*x*Cr-4Ti-0.15Y alloys are likely to correspond to the loss of hardening due to DSA.

Figure 6 shows absorbed energies from -196 ºC to RT. In the present study, ductile-to-brittle transition temperature (DBTT) is defined as the temperature where the absorbed energy is half of the upper-shelf energy (USE). Table 2 summarizes USEs and DBTTs for the alloys tested in the present study. DBTTs for V-4Cr-4Ti and V-4Cr-4Ti-0.15Y alloys were below -196 ºC. DBTTs for V-6Cr-4Ti-0.15Y and V-10Cr-4Ti-0.15Y alloys were estimated as -194 and -130 ºC, respectively.

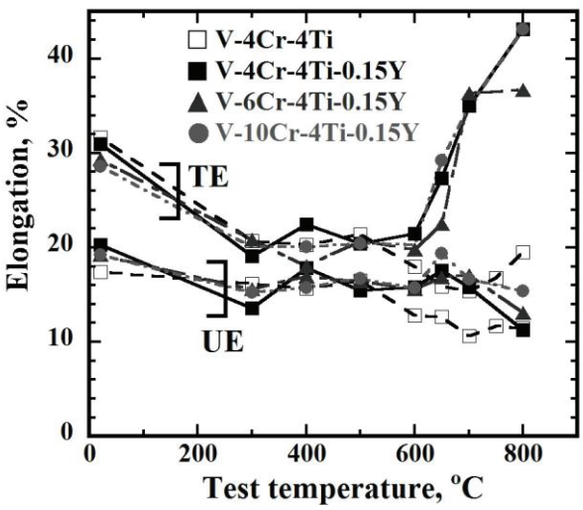

Fig. 4. Dependence of uniform elongation (UE) and total elongation (TE) on test temperatures.

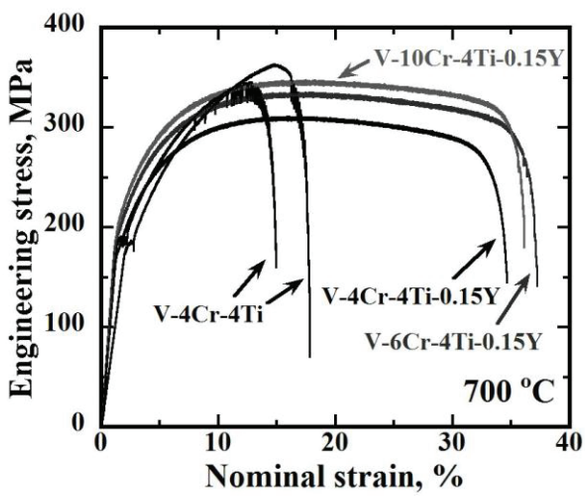

Fig. 5. Tensile stress-strain curves for the alloys at 700 ºC. Tensile tests for V-4Cr-4Ti alloy were carried out twice in order to confirm the reproducibility of serrations.

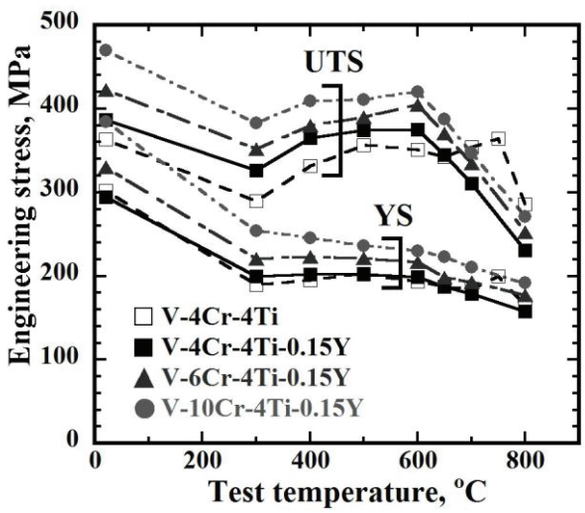

Fig. 3. Dependence of yield stress (YS) and ultimate tensile strength (UTS) on test temperatures.

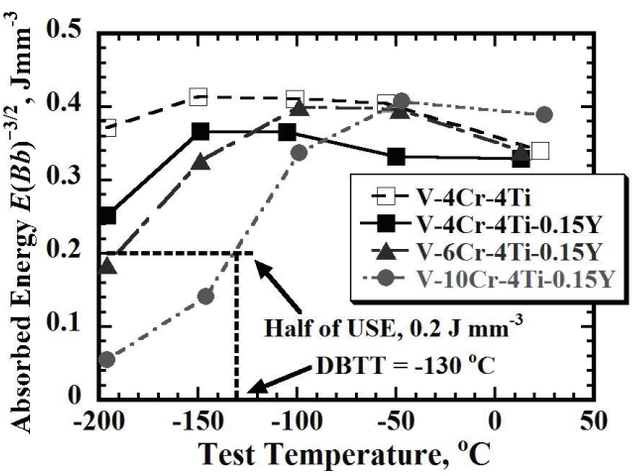

Fig. 6. Absorbed energies in the Charpy impact tests. These energies are normalized by specimen width (B = 1.5 mm) and ligament size (b = 1.2 mm).

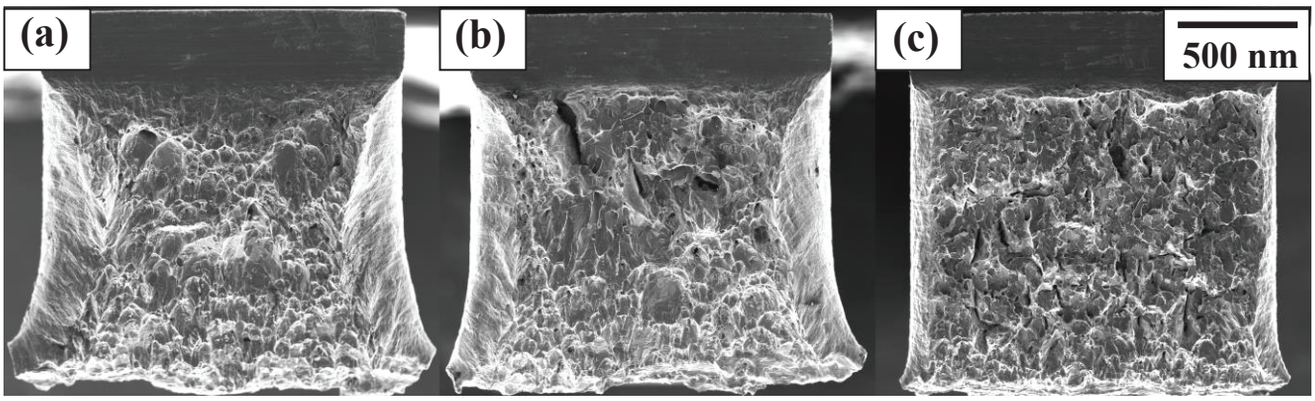

Fig. 7. SEM images for fracture surface tested at -196 ºC. (a) V-4Cr-4Ti-0.15Y, (b) V-6Cr-4Ti-0.15Y, (c) V-10Cr-4Ti-0.15Y.

Table 2 Summary of Charpy impact properties.

Code	USE (J/mm^3)	DBTT (ºC)
V-4Cr-4Ti	0.39	Below -196
V-4Cr-4Ti-0.15Y	0.35	Below -196
V-6Cr-4Ti-0.15Y	0.38	-194
V-10Cr-4Ti-0.15Y	0.40	-130

Figure 7 presents SEM images of the fracture surfaces of V-*x*Cr-4Ti-0.15Y alloys tested at -196 ºC. The fracture surface of V-4Cr-4Ti-0.15Y alloy exhibited good ductility. The fracture surface of V-6Cr-4Ti-0.15Y alloy was a mixture of ductile fractures with dimples and brittle fractures with secondary cracks. The fracture surface of V-10Cr-4Ti-0.15Y alloy indicated fully brittle fracture characterized by cleavage and secondary crack with random directions.

4. Discussions

V-10Cr-4Ti-0.15Y alloy has UTS at 700 ºC and YS approximately equal to and higher than those of V-4Cr-4Ti alloy, respectively. The Cr addition provides strengthening as a substitutional solute in vanadium alloys. In order to compensate for the decrease of high-temperature strength due to the loss of hardening by DSA, the Cr addition is an effective method, as shown in Fig. 3. Because it is known that the change in UTS at high-temperature has a close relation with thermal creep properties, it is necessary to investigate the creep properties of V-10Cr-4Ti-0.15Y alloy.

Figure 8 summarizes the dependence of DBTT for V-*x*Cr-(4-5)Ti and V-*x*Cr-4Ti-0.15Y alloys on Cr content [10, 15]. Higher Cr content increases DBTT of V-*x*Cr-(4-5)Ti alloys significantly. However, V-10Cr-4Ti-0.15Y alloy has lower DBTT than those of V-*x*Cr-(4-5)Ti alloys with $x > 9$ wt.%. It seems that the factors contributing to DBTT are not only the solution hardening of Cr but also the difference in precipitation behavior. Sakai et al. [10] clarified that high DBTTs of V-*x*Cr-4Ti alloys with $x > 10$ wt.% were caused by high flow stress due to solution hardening of Cr, and by initiation of crack formation due to the large Ti-rich precipitates (about 500-1000 nm). The contamination of gaseous impurities such as O may result in the formation of the large Ti-rich precipitates to act as crack initiation sites. Therefore, the reasons for favorable impact properties of V-10Cr-4Ti-0.15Y alloy are considered to be as follows: (1) The purification could suppress the formation of the large Ti-rich precipitates because V-*x*Cr-4Ti-0.15Y alloys examined in this study have low level of C, O and N content. (2) The formation of Y_2O_3 inclusions during the melting process [9, 14] could further reduce O content in the matrix, and then suppress the formation of the large Ti-rich precipitates. Further study of microstructural examinations is necessary to determine the size, number density and distribution morphology of precipitates in V-10Cr-4Ti-0.15Y alloy.

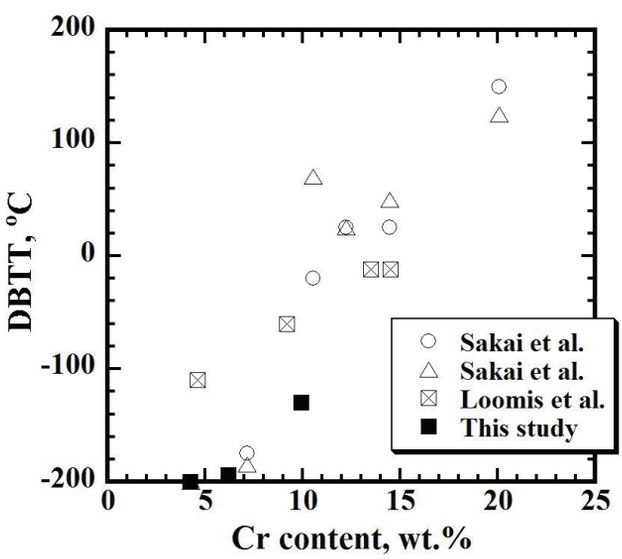

Fig. 8. Dependence of DBTT for V-*x*Cr-(4-5)Ti and V-*x*Cr-4Ti-0.15Y alloys on Cr content. Open circles and open triangles represent V-*x*Cr-4Ti alloys annealed at heat treat conditions to obtain a mean grain size of 17 μm, and at 950 ºC [10]. Open squares with cross represent V-*x*Cr-5Ti alloys annealed at 1125 ºC [15]. Closed squares represent V-*x*Cr-4Ti-0.15Y alloys annealed at 950 ºC (this study).

5. Summary

High-temperature tensile properties and low-temperature impact properties of high-Cr V-*x*Cr-4Ti-0.15Y alloys (x = 6, 10 wt.%) were examined.

1) V-10Cr-4Ti-0.15Y alloy had UTS at 700 °C and YS approximately equal to and higher than those of V-4Cr-4Ti alloy, respectively. High Cr addition is shown to compensate for the decrease in the high-temperature strength by purification and Y addition.
2) V-10Cr-4Ti-0.15Y alloy has more favorable impact properties than those of previous V-*x*Cr-(4-5)Ti alloys with x > 9 wt.%. It is proposed that purification and Y addition may suppress the formation of the large Ti-rich precipitates to act as crack initiation sites.

Acknowledgement

The authors are grateful to Prof. K. Fukumoto of Fukui Univ. for the support in the preparation of the specimens and the fruitful discussions. This work was supported by Grant-in-Aid for Scientific Research (C), (2013-2015) 25420889.

References

[1] T. Muroga, Comprehensive Nuclear Materials **4**, 391 (2012).
[2] S.J. Zinkle and N.M. Ghoniem, Fusion Eng. Des. **51**, 55 (2000).
[3] H.M. Chung, B.A. Loomis and D.L. Smith, J. Nucl. Mater. **239**, 139 (1996).
[4] M.L. Grossbeck, J.F. King, D.J. Alexander, P.M. Rice and G.M. Goodwin, J. Nucl. Mater. **258**, 1369 (1998).
[5] N.J. Heo, T. Nagasaka and T. Muroga, J. Nucl. Mater. **325**, 53 (2004).
[6] K. Fukumoto, H. Matsui, Y. Candra, K. Takahashi, H. Sasanuma, S. Nagata and K. Takahiro, J. Nucl. Mater. **283**, 535 (2000).
[7] M. Satou, T. Chuto and K. Abe, J. Nucl. Mater. **283**, 367 (2000).
[8] T. Chuto, M. Satou, A. Hasegawa, T. Muroga and N. Yamamoto, Effects of Radiation on Mater. ASTM STP-1447, 693 (2004).
[9] T. Miyazawa, T. Nagasaka, Y. Hishinuma, T. Muroga, Y. Li, Y. Satou, S. Kim and H. Abe, J. Nucl. Mater. **442**, S341 (2013).
[10] K. Sakai, M. Satou, M. Fujiwara, K. Takahashi, A. Hasegawa and K. Abe, J. Nucl. Mater. **329**, 457 (2004).
[11] T. Nagasaka, T. Muroga, M. Imamura, S. Tomiyama and M. Sakata, Fusion Technol. **39**, 659 (2001).
[12] T. Nagasaka, N.J. Heo, T. Muroga and M. Imamura, Fusion Eng. Des. **61**, 757 (2002).
[13] T. Chuto, T. Nagasaka, T. Muroga, M. Satou, K. Abe, T. Shibayama, S. Tomiyama and M. Sakata, J. Japan Inst. Metals **64**, 743 (2000).
[14] T. Nagasaka, T. Muroga, T. Hino, M. Satou, K. Abe, T. Chuto and T. Iikubo, J. Nucl. Mater. **367**, 823 (2007).
[15] B.A. Loomis, H.M. Chung, L.J. Nowicki and D.L. Smith, J. Nucl. Mater. **212**, 799 (1994).